Thermally activated delayed fluorescence carbazole - triazine dendrimer with bulky substituents

Ikebe, Hiroki
Interdisciplinary Graduate School of Engineering Sciences Kyushu University

Nakao, Kohei
Institute for Materials Chemistry and Engineering, Kyushu University

Hisamura, Eri
Institute for Materials Chemistry and Engineering, Kyushu University

Furukori, Minori

他

出版情報：Aggregate. 5 (1), 2023-08-17. Wiley
バージョン：

Received: 30 May 2023 | Revised: 27 July 2023 | Accepted: 30 July 2023

DOI: 10.1002/agt2.405

Aggregate Open Access WILEY

RESEARCH ARTICLE

Thermally activated delayed fluorescence carbazole-triazine dendrimer with bulky substituents

Hiroki Ikebe[1] | **Kohei Nakao**[2] | **Eri Hisamura**[2] | **Minori Furukori**[3,4] | **Yasuo Nakayama**[3,4] | **Takuya Hosokai**[3,4] | **Minlang Yang**[5] | **Guanting Liu**[5] | **Takuma Yasuda**[5] | **Ken Albrecht**[2]

[1]Interdisciplinary Graduate School of Engineering Sciences, Kyushu University, Fukuoka, Japan

[2]Institute for Materials Chemistry and Engineering, Kyushu University, Kasuga, Japan

[3]Department of Pure and Applied Chemistry, Graduate School of Science and Technology, Tokyo University of Science, Noda, Chiba, Japan

[4]National Metrology Institute of Japan (NMIJ), National Institute of Advanced Industrial Science and Technology (AIST), Tsukuba, Ibaraki, Japan

[5]Institute for Advanced Study, Kyushu University, Nishi-ku, Fukuoka, Japan

Correspondence
Takuya Hosokai, National Metrology Institute of Japan (NMIJ), National Institute of Advanced Industrial Science and Technology (AIST), 1-1-1 Higashi, Tsukuba, Ibaraki 305-8565, Japan.
Email: t.hosokai@aist.go.jp

Ken Albrecht, Institute of Materials Chemistry and Engineering, Kyushu University, 6-1 Kasuga Koen, Kasuga 816-8580, Japan.
Email: albrecht@cm.kyushu-u.ac.jp

Funding information
Ministry of Education, Culture, Sports, Science and Technology, Grant/Award Number: ARIM/JPMXP1222JI0040; Japan Society for the Promotion of Science, Grant/Award Numbers: KAKENHI/JP20KK0316, KAKENHI/JP21H05405, KAKENHI/JP22H02055, KAKENHI/JP23H02026, KAKENHI/JP23H03966, KAKENHI/JP20H02801

Abstract
Carbazole-triazine dendrimers with a bulky terminal substituent were synthesized, and the thermally activated delayed fluorescence (TADF) property was investigated. Compared to unsubstituted carbazole dendrimers, dendrimers with bulky terminal substituents showed comparable to better photoluminescence quantum yields (PLQY) in neat films. Phenylfluorene (PF)-substituted dendrimers showed the highest PLQY of 81%, a small ΔE_{st} of 0.06 eV, and the fastest reverse intersystem crossing (RISC) rate of $\sim 1 \times 10^5$ s^{-1} compared to other dendrimers. Phosphorescence measurements of dendrimers and dendrons (fragments) indicate that the close proximity of the triplet energy of phenylfluorene-substituted carbazole dendrons (^{3}LE) to that of phenylfluorene-substituted dendrimers (^{1}CT, ^{3}CT) contributes to RISC promotion and improves TADF efficiency. Terminal modification fine-tunes the energy level and suppresses intermolecular interactions, and this study provides a guideline for designing efficient solution-processable and non-doped TADF materials.

KEYWORDS
dendrimer, OLED, TADF

1 | INTRODUCTION

Thermally activated delayed fluorescence (TADF)[1] materials, which are inexpensive and highly efficient alternatives to fluorescent and phosphorescent materials as light-emitting materials for organic light-emitting diodes (OLEDs),[2] have been attracting attention and were being vigorously studied for higher efficiency in terms of photoluminescence quantum yield (PLQY),[3] reverse intersystem crossing (RISC) rate,[4] narrow emission bandwidth,[5] and device stability.[6] The design concept of TADF materials is that the intramolecular separation of highest occupied molecular orbital (HOMO) and lowest unoccupied molecular orbital (LUMO) results in a small ΔE_{ST} (energy difference between singlet and triplet excited states). The importance of controlling higher triplet state (Tn) energy levels to increase the RISC rate has also been pointed out through an increase in the spin–orbit coupling (SOC) between the charge-transfer singlet (^{1}CT) and locally excited triplet (^{3}LE) states through the Tn levels.[7] Reducing the energy gap between the charge-transfer singlet

(^{1}CT), charge-transfer triplet (^{3}CT), and locally excited triplet (^{3}LE) states maximizes the SOC and RISC processes. Small ΔE_{ST} and large SOC are believed to achieve a fast RISC of the triplet exciton to the singlet state at room temperature and enable an internal quantum efficiency (IQE) of 100% in an OLED device.

A large fraction of the reported TADF OLEDs have been fabricated by the vacuum deposition method employing low-molecular-weight materials.[8] However, there are several problems with the restricted thermal stability of the OLED materials, low material utilization during deposition, manufacturing complexity, and time and energy consumption. OLED device fabrication methods using solution process are gaining attention to address these issues and reduce product costs.[9] Employing a non-doped emissive material layer can also simplify the device fabrication process because optimization (selection) of the host, doping concentration, and consideration of the solubility is unnecessary and potential thread of phase separation can be avoided.[10] In contrast to the vacuum evaporation method, TADF materials that are applicable to solution process can reduce costs by increasing the device area and productivity and saving production energy. OLED materials are required to form amorphous, smooth films and have sufficient solubility for ink preparation. Ordinary low-molecular-weight materials are not suitable for the solution process. Solution-processable TADF materials must also meet these requirements, and low- and medium-molecular materials with bulky structures,[11] polymers,[12] and dendrimers[13] have been considered. Dendrimers[14] are polymers with absolute molecular weight and well-defined chemical structures and have been employed as OLED materials due to their high purity, thermal stability, structural designability, and high solubility.[15] Furthermore, the structure with a large steric hindrance can prevent aggregation caused quenching (ACQ) by isolating chromophores at the core. Carbazole dendrimers have been widely studied as solution-processable OLED materials such as hole transport materials,[16] host materials,[17] and single-component emitting materials[18] because of their hole-transporting character, high triplet energy, cross-linking ability, and unique polarized electronic structure[19] that makes them also suitable as donor units in TADF materials.[20]

Triphenyltriazine (TAZ) is a commonly used electron acceptor for TADF emitters in combination with various donors,[21] including carbazole dendrimers.[13a,22] The first TADF dendrimers were second- to fourth-generation carbazole-triazine dendrimers, and these dendrimers have very small ΔE_{ST} due to the separation of the outer-layer localized HOMO and LUMO distributing on the core triazine. The PLQY in solution is nearly 100% but in neat film lower than 50% indicating the ACQ. Generally, to decrease the concentration quenching, it has been shown that the introduction of bulky substituents or spacers reduces intermolecular interactions and suppresses ACQ.[23]

The recent non-doped solution-process OLEDs using TADF dendrimers with relatively high PLQY up to over 80% in the neat film have been rarely reported.[22c,24] In the previous study with carbazole-benzophenone dendrimer, adamantane and tetraphenylphenyl group was shown to be insufficient to suppress ACQ, and the terminal structure strongly affected the TADF properties.[25] In this study, we have focused on carbazole-triazine dendrimer that, previously, a *tert*-butyl group had been introduced as a bulky substituent but was not sufficient to suppress ACQ.[22a] Here we will report a carbazole-triazine dendrimer with bulkier substituents to inhibit ACQ and report a top-class PLQY as a non-doped TADF dendrimer (81%).

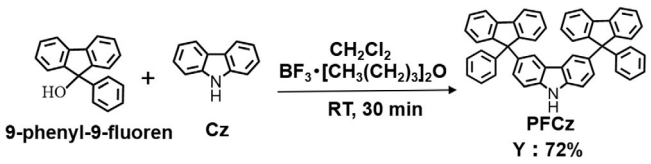

FIGURE 1 The synthesis of 9-phenylfluorene-substituted carbazole.

2 | RESULTS AND DISCUSSION

2.1 | Synthesis

Three TAZ core carbazole dendrimers with bulky substituents (Ad, adamantane; TPPh, tetraphenylphenyl; PF, phenylfluorene) were designed and synthesized using copper-catalyzed N-arylation as the key reaction (Figures 1 and 2).[26] The Ad-[27] and TPPh-[28] modified carbazoles were synthesized by Friedel–Crafts type aromatic electrophilic substitution reaction and Diels–Alder reaction according to the literature. The PF-modified carbazole was synthesized by Friedel–Crafts type aromatic electrophilic substitution reaction of 9-phenyl-9-fluorene and carbazole.[29] The G2 dendron was synthesized via copper-catalyzed N-arylation[19a] of the modified carbazole and silyl-protected 3,6-diiodocarbazole (I2CzTBS) and following deprotection of the silyl group by tetrabutylammonium fluoride (TBAF). Dendrons (Ad, TPPh, and PF) were reacted with 2,4,6-tris(4-iodophenyl)-1,3,5-triazine under N-arylation condition at 160°C (microwave) to afford the corresponding carbazole TAZ dendrimers (AdG2TAZ, TPPhG2TAZ, and PFG2TAZ). Unsubstituted G2TAZ was also synthesized according to the literature.[13a] G2TAZ, TPPhG2TAZ, and PFG2TAZ showed good solubility (>5 mg/mL) in toluene, THF, and chloroform and poor solubility in cyclohexane, acetone, and DMSO. AdG2TAZ showed good solubility in THF, poor solubility in cyclohexane, and insoluble in acetone and DMSO (the saturated solution did not show detectable fluorescence). New carbazole-triazine dendrimers with bulky substituents were successfully synthesized, and all new compounds were characterized by ^{1}H and ^{13}C NMR, MALDI-TOF-MS.

2.2 | Film formation property

THF solutions of AdG2TAZ and chloroform solutions of G2TAZ, TPPhG2TAZ, and PFG2TAZ were spin coated onto Si substrates to prepare films (5 mg/mL THF solution), and AFM images were obtained (Figures S1, S3, S5, and S7). The images of AdG2TAZ show some flat deposition areas (0.8 × 0.8 μm), but on a larger scale, the surface was rough, and sphere aggregates were observed (5 × 5 μm). The solubility of AdG2TAZ is lower, and 5 mg/mL chloroform could not be prepared. The 5 mg/mL THF could be prepared, and the

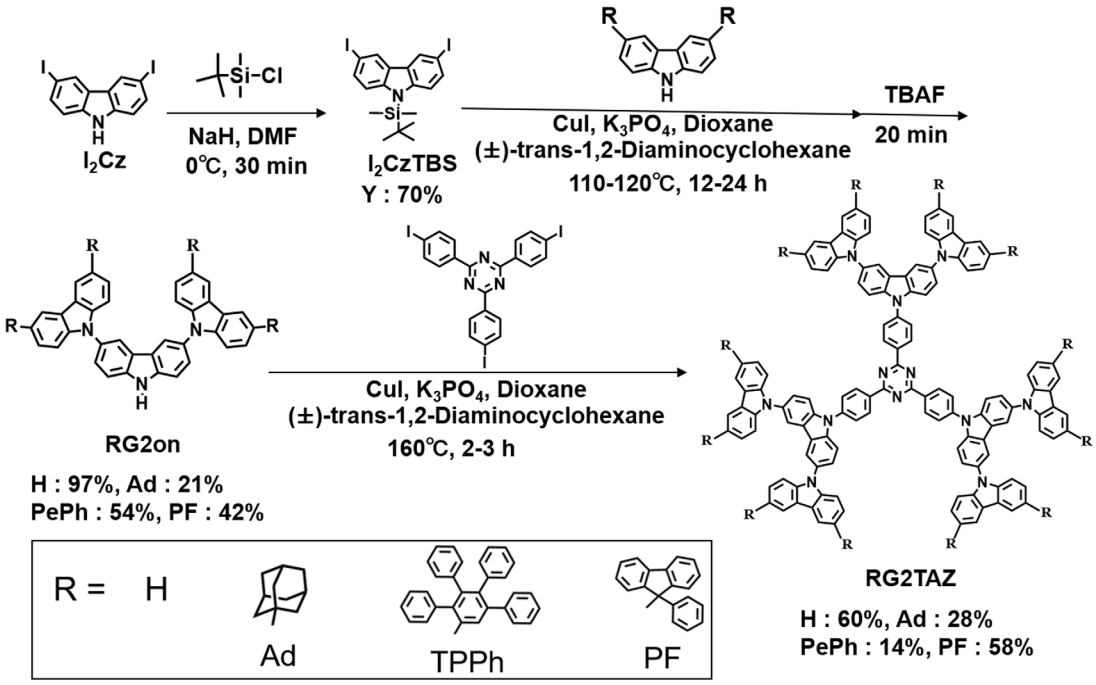

FIGURE 2 Synthesis of carbazole G2 dendrons and triphenyltriazine core dendrimers.

relatively lower solubility of AdG2TAZ will lead to aggregation and precipitation during the drying process. Roughness was calculated from the enlarged image. Root mean square (RMS) was 0.27 nm (0.8 × 0.8 μm) for the flat deposition area and 70.19 nm (5 × 5 μm) for the whole image, including the aggregates. This indicates that AdG2TAZ is not favorable for film deposition in devices. On the other hand, all other dendrimer films were found to have smooth surfaces in both the wide (5 × 5 μm) and narrow (2 × 2 μm) ranges. RMS was 0.44, 0.28 nm (G2TAZ); 0.37, 0.36 nm (TPPhG2TAZ); and 0.32, 0.29 nm (PFG2TAZ) for the respective ranges. The same trend was observed when a higher boiling point toluene solution (5 mg/mL) was used to prepare the film (Figures S2, S4, S6, and S8). Note that AdG2TAZ was used as a dispersion due to the low solubility. G2TAZ, TPPhG2TAZ, and PFG2TAZ have good film-forming properties for future device fabrication, but AdG2TAZ has insufficient solubility in common organic solvents and easily formed aggregates.

2.3 | Thermal property

The thermal stability of the dendrimers was checked with thermogravimetric (TG) analysis (Figure S9). The 5% weight loss temperatures ($Td_{5\%}$) of dendrimers were 588°C (G2TAZ), 524°C (AdG2TAZ), 588°C (TPPhG2TAZ), and 583°C (PFG2TAZ). differential TG (DTG) curves indicate that the fully aromatic dendrimers start to degrade at around 540°C, comparable to previously reported carbazole-based dendrimers.[13a] In contrast, AdG2TAZ started to degrade at about 450°C. The degradation of AdG2TAZ starting at 450°C and lower Td5% can be attributed to the partial degradation of the aliphatic adamantane group.[30] Although aliphatic adamantane substitution lowers the degradation temperature of the dendrimers, all dendrimers have sufficiently high thermal stability for applications in electronic devices.

2.4 | Electrochemical property

The cyclic voltammogram of each dendrimer was obtained in dichloromethane or THF (Figure S11). Unsubstituted G2TAZ showed oxidative electropolymerization behavior that is typical to 3,6-unsubstituted carbazole derivatives.[19d,31] On the other hand, 3,6-substituted dendrimers showed two stable redox waves that did not change after 5 cycles. This stable oxidation behavior will be an advantage under device operation conditions, that is, stability during hole transportation. The redox waves can be attributed to the oxidation of one of the outermost carbazoles of the dendron, and the second oxidation can be attributed to the oxidation of the remaining carbazole unit at the outermost layer.[19b] Due to the difference in the diffusion constant of each dendrimer (suggested by the difference in current), it is difficult to determine the accurate number of electrons involving oxidation. In a previous report, multi-electron oxidation and interaction between carbazole moieties in the carbazole dendron are reported.[19b] Three dendrons in one dendrimer should be independently oxidized due to the limited conjugation. Therefore, each oxidation peak is assumed to be three electron-transfer reactions. The electrochemical behavior guarantees that new dendrimers are stable hole-transporting materials.

3 | QUANTUM CHEMICAL CALCULATIONS

Density functional theory (DFT) and time-dependent density functional theory (TD-DFT) calculations were performed to determine the electronic structure of dendrimers. In addition, natural transition orbital (NTO) pairs for the lowest singlet and triplet state transitions in toluene were investigated (Figure S10). The calculated HOMO/LUMO levels were −5.40/−2.62, −5.16/−2.53, −5.16/−2.57, and −5.24/−2.54

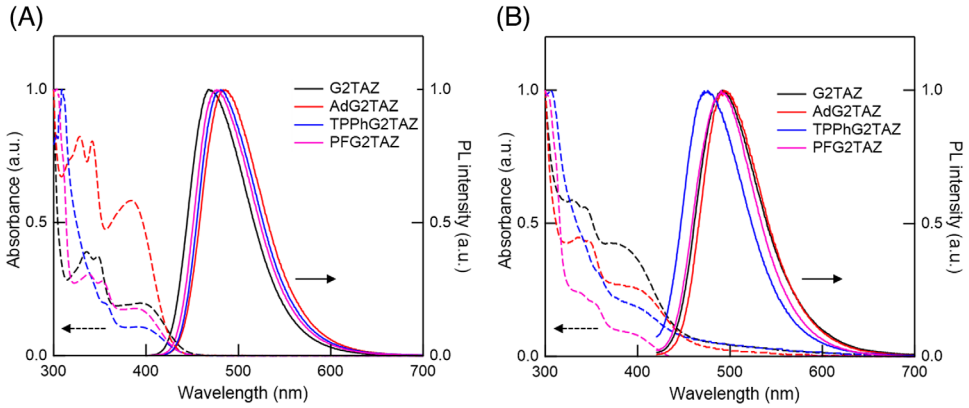

FIGURE 3 UV–vis spectra and PL spectra of dendrimers (A) toluene solution and (B) neat film.

eV for G2TAZ, AdG2TAZ, TPPhG2TAZ, and PFG2TAZ, respectively (Table S1). The calculated HOMO levels were higher than the values determined by cyclic voltammetry (CV) and atmospheric photoelectron spectroscopy (PYS) (Figure S11, Tables S2 and S3). Calculations often include errors, and the absolute value is not accurate, but the trend was similar to the experimental values. The higher HOMO levels of the substituted dendrimers than of the unsubstituted G2TAZ reflect the increased electron-donating nature of the substituents. In particular, AdG2TAZ has a higher HOMO level due to its aliphatic substituents. The ΔE_{st} of all dendrimers was small (0.06–0.11 eV), and the NTO shows that the excited state has a CT character indicating their potential as TADF emitters (Table S1).

4 | PHOTOPHYSICAL PROPERTIES

UV–vis absorption and PL spectra of the synthesized dendrimers in toluene and in the neat film state were measured (Figure 3). The UV–vis spectra showed a broad and weak absorption band around 390 nm both in toluene and the film. This absorption band was not observed in the UV–vis spectra of the dendrimer fragments (carbazole and TAZ) (Figure S12) and was attributed to charge-transfer (CT) absorption from carbazole to TAZ. The PL spectra were observed in toluene at 468 nm (G2TAZ), 484 nm (AdG2TAZ), 481 nm (TPPhG2TAZ), and 477 nm (PFG2TAZ) and in neat films at 492 nm (G2TAZ), 493 nm (AdG2TAZ), 476 nm (TPPhG2TAZ), and 490 nm (PFG2TAZ). Both PL spectra were broad, attributed to emission from CT excited states. The large bathochromic shifts in G2TAZ, AdG2TAZ, and PFG2TAZ can be explained by the changes in the medium polarity and intermolecular interaction. On the other hand, the slight hypsochromic shift in TPPhG2TAZ may be due to the similar environment in solution and in the neat film due to the substituents consisting of many benzene rings as in toluene. The excited state CT character of all dendrimers was confirmed, and the behavior in the solution and the neat film showed different behaviors depending on the dendrimer.

The PL spectra were also measured in various solvents with different polarities to confirm the excited state CT character (Figure S13, Tables S4–S7). Large bathochromic shifts of the PL maxima were observed with increasing polarity. In DMSO, the most polar solvent in the measurement, emission was observed at 576 nm (G2TAZ), 552 nm (TPPhG2TAZ), and 580 nm (PFG2TAZ). The PL spectrum of AdG2TAZ could not be detected in DMSO due to poor solubility. Lippert–Mataga plot showed that the emission peak energy is linearly related to the solvent polarity parameter (E_T^N),[32] indicating that the emission is from a single excited state. All dendrimers were confirmed to emit from a single CT excited state.

The PLQY was measured in toluene and neat film (Table 1). The PLQY in toluene solutions of each dendrimer was 72% (G2TAZ), 67% (AdG2TAZ), 74% (TPPhG2TAZ), and 77% (PFG2TAZ) under atmospheric conditions, but increased to nearly 100% for all dendrimers in a nitrogen atmosphere. This suggests the contribution of a long-lived excited state, such as a triplet excited state that is easily quenched by oxygen diffusion, and the PL can be attributed to TADF or phosphorescence. The PLQY of neat films under a nitrogen atmosphere was 54% (G2TAZ), 65% (AdG2TAZ), 51% (TPPhG2TAZ), and 81% (PFG2TAZ). In general, ACQ takes place in the solid state of luminophores. The PLQY data of the films indicates that even for bulky substituents, the ACQ cannot be perfectly avoided, but the PF group serves as the best substituent by inhibiting intermolecular interactions. The PLQY revealed that all dendrimers have a long-lifetime component that is quenched with oxygen, and the concentration quenching can be largely suppressed by locating the bulky PF group at the terminal of the dendrimer.

From the onset of the fluorescence and phosphorescence spectra at 77 K, the energy levels of S_1 and T_1 excited states were determined, and ΔE_{st} was calculated (Figures S14 and S15). The ΔE_{st} in neat films were 0.11 (G2TAZ), 0.09 (AdG2TAZ), 0.17 (TPPhG2TAZ), and 0.06 eV (PFG2TAZ), respectively, which are sufficiently small to expect TADF expression. The smallest ΔE_{st} of PFG2TAZ among the new dendrimers reflects a large PLQY.

Transient PL decay curves were measured in toluene and in neat films to confirm the TADF expression of dendrimers (Figure 4, Figure S16, Table 1[33]); the apparatus and method are described in the literature.[34] The PL lifetimes clearly indicate the presence of a short-lived component of the order of ns and a long-lived component of the order of μs. The lifetimes of the delayed components in toluene and in neat films were G2TAZ (17, 5.5 μs), AdG2TAZ (10, 9.2 μs), TPPhG2TAZ (1.7, 7.7 μs), and PFG2TAZ (36, 8.6 μs). The lifetime and the similarity of the emission spectra between the prompt and delayed components indicate that the long-lifetime component is attributed to

TABLE 1 Photophysical properties of dendrimers in toluene solution and neat films at 300 K.

	State	Φ_{PL} (air/degassed or in vacuum)	τ_F [ns]	τ_{TADF} [μs]	Φ_F	Φ_{TADF}	k_F (10^7) [s^{-1}][a]	$k_{IC,T}$ (10^4) [s^{-1}][a]	k_{ISC} (10^7) [s^{-1}][a]	k_{RISC} (10^4) [s^{-1}][a]	ΔE_{st} [eV]
G2TAZ	Solution	72/98	10	17	97.1	0.9	9.7	4.1	0.29	2.0	0.16
	Neat film	41/54	12[b]	5.5[b]	47	7.0	4.0	16	4.5	5.1	0.11
AdG2TAZ	Solution	67/94	13	10	91.1	2.9	7.0	6.8	0.68	3.6	0.11
	Neat film	45/65	15[b]	9.2[b]	58	7.0	3.8	9.1	2.7	3.1	0.09
TPPhG2TAZ	Solution	74/95	12	1.7	94.8	0.2	7.9	57	0.43	2.4	0.16
	Neat film	47/51	11[b]	7.7[b]	50.1	0.9	4.7	13	4.6	0.4	0.17
PFG2TAZ	Solution	77/99	11	36	92.3	6.7	8.6	0.4	0.71	2.6	0.16
	Neat film	50/81	16[b]	8.6[b]	64.3	16.7	4.1	6.2	2.2	8.4	0.06

[a]Fluorescence decay rate (k_F), internal conversion decay rate from T_1 to S_0 ($K_{IC,T}$), intersystem crossing decay rate from S_1 to T_1 (k_{ISC}), and reverse intersystem crossing decay rate from T_1 to S_1 (k_{RISC}) are calculated from Φ_{PL}, Φ_F, Φ_{TADF}, τ_F , and τ_{TADF} according to [ref 32], where non-radiative decay from S_1 to S_0 and radiative decay from T_1 to S_0 are assumed to be zero.

[b]An average lifetime calculated by $\tau_{av} = \Sigma A_i\tau_i^2 / \Sigma A_i\tau_i$, where A_i is the pre-exponential for lifetime τ_i.

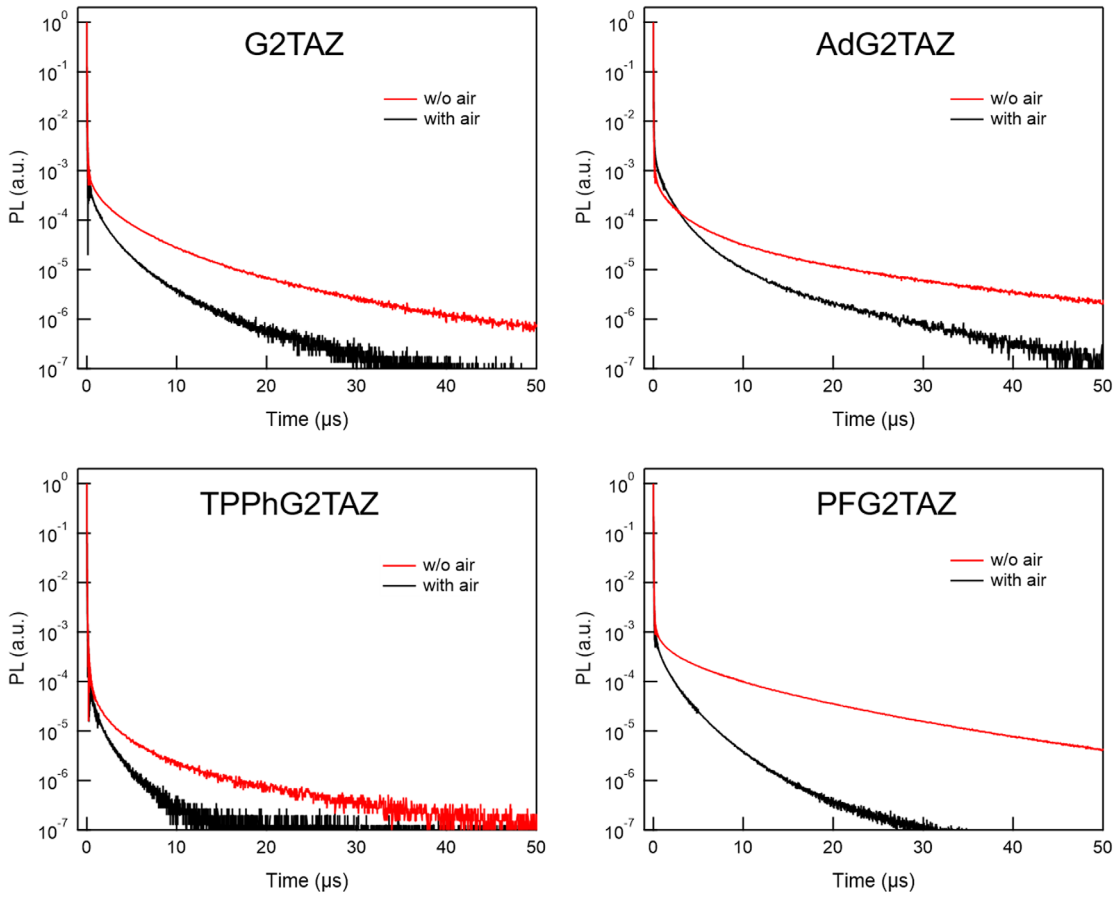

FIGURE 4 Transient PL decay profiles of G2TAZ, AdG2TAZ, TPPhG2TAZ, and PFG2TAZ neat film at 300 K.

TADF. The temperature dependence of the long-lifetime component (Figure S17) supports this assignment. At higher temperatures, the lifetime of the long-lifetime component decreases due to the increase of the k_{RISC} rate, similar to previous reports[13a,22a]. The calculated rate constants for RISC were classified into three types when going from solution to film, that is, larger (G2TAZ, PFG2TAZ), almost the same (AdG2TAZ), and smaller (TPPhG2TAZ). This can be related to the degree of decrease in ΔE_{st} when changing from toluene to neat films. ΔE_{st} in solution and neat films were 0.16, 0.11 (G2TAZ), 0.11, 0.09 (AdG2TAZ), 0.16, 0.17 (TPPhG2TAZ), 0.16, and 0.06 eV (PFG2TAZ). The change in ΔE_{st} from solution to neat film was significantly decreased for G2TAZ and PFG2TAZ, with a slight decrease for AdG2TAZ. TPPhG2TAZ slightly increased, and ΔE_{st} was larger than the other dendrimers. This behavior matches the trend of the lifetime of the TADF component, that is, when ΔE_{st} is smaller lifetime will be shorter. The $k_{IC,T}$ (non-radiative deactivation constant from the triplet) was the smallest for PFG2TAZ in both toluene and neat films. The highest PLQY of PFG2TAZ

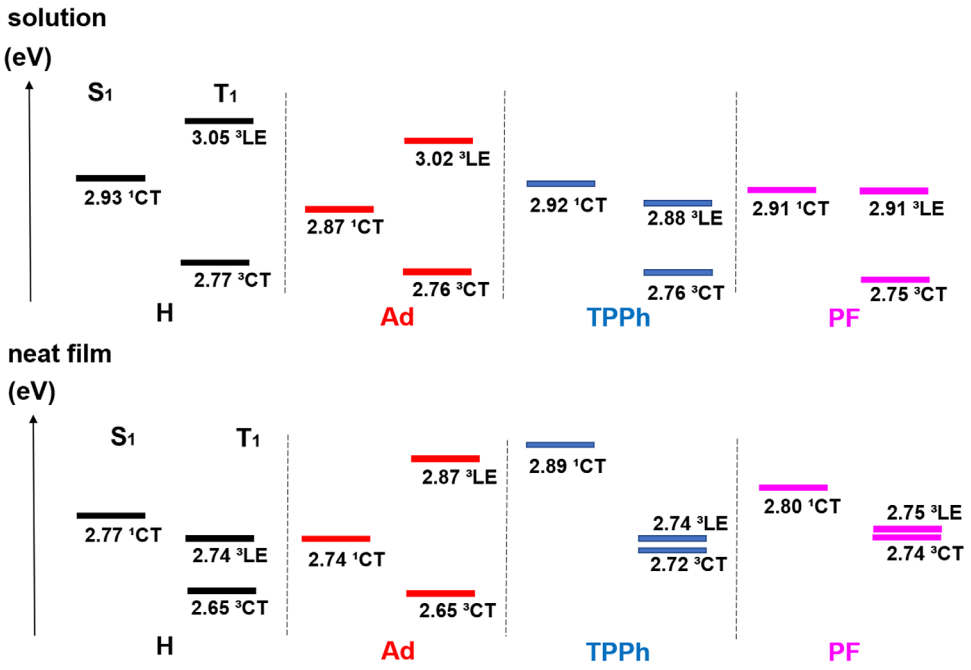

FIGURE 5 Energy diagram of excited states of G2TAZ, AdG2TAZ, TPPhG2TAZ, and PFG2TAZ in toluene solution and neat film.

in neat films is supported by the largest k_{RISC} and the smallest $k_{IC,T}$. On the other hand, in TPPhG2TAZ, the k_{RISC} in neat films is one order of magnitude smaller than other new dendrimers, and the Φ_{TADF} shows little TADF characteristics. This may be due to the large ΔE_{st} and the presence of other deactivation pathways related to benzene ring rotation, as previously reported.[25] The TADF expression was confirmed, and these data suggest that the terminal modification of the dendrimer strongly affects the TADF property.

To further understand the effect of terminal structure on TADF efficiency, the energy levels ^{1}CT and ^{3}CT of the dendrimer and ^{3}LE from the donor unit (carbazole dendron) were investigated. Note that the triplet energy of the triazine core is higher than the carbazole dendron.[35] ^{3}LE mediation plays an important role in efficient RISC processes by increasing the SOC between the triplet and singlet states. In general, efficient TADF (RISC) can be expected by decreasing the gap between ^{3}CT and ^{3}LE. The energy levels of ^{3}LE were determined from the onset of fluorescence and phosphorescence spectra of frozen toluene solutions and neat films of the dendron at 77 K (Figure 5, Figures S18 and S19). The energy difference ^{3}LE − ^{3}CT is defined as $\Delta T - T$. In toluene, $\Delta T - T$ were +0.28 (G2TAZ), +0.26 (AdG2TAZ), +0.12 (TPPhG2TAZ), and +0.16 eV (PFG2TAZ). Thus, ^{3}LE was found to be located above ^{3}CT. The energy levels are far apart and may not be considered to be an effective arrangement for the RISC process in the toluene solutions. In fact, AdG2TAZ exhibits smallest ΔE_{st} (0.11 eV) and largest k_{RISC} (3.6×10^4 s^{-1}), while other dendrimers possess the larger ΔE_{st} (0.16 eV) and comparably smaller k_{RISC} ($2.0–2.6 \times 10^4$ s^{-1}). In the neat films, $\Delta T - T$ values of +0.09 (G2TAZ), +0.22 (AdG2TAZ), +0.02 (TPPhG2TAZ), and +0.01 eV (PFG2TAZ) have been observed. In G2TAZ and PFG2TAZ, the energy level configuration was ideal for accelerating the RISC process due to their close energetic proximity. In TPPhG2TAZ, even though the $\Delta T - T$ was small, the ΔE_{st} was larger than other dendrimers, which reduces k_{RISC}. Also, in AdG2TAZ, ^{3}LE is located further above ^{1}CT, which is presumed that it does not contribute to accelerating RISC. This explains the reason why k_{RISC} of AdG2TAZ is similar in toluene and neat film. PFG2TAZ not only has a small ΔE_{st}, but also allows for an efficient RISC process mediated by ^{3}LE in neat film.

Three dendrimers (G2TAZ, TPPhG2TAZ, and PFG2TAZ) were evaluated as emitting layers in OLED devices, although AdG2TAZ could not be evaluated due to its poor solubility and film-forming property (Figures S20 and S21, Table S8). OLED devices with the configuration of ITO/PEDOT-PSS/PVK/dendrimer/PPF/B3PyPB/Liq/Al were fabricated and evaluated. PEDOT-PSS was a hole-injection layer, PVK was an electron blocking layer, dendrimer neat film was the emitting layer, PPF was hole blocking layer, and B3PyPB was electron-transporting layer. PEDOT-PSS, PVK, and dendrimer layers were fabricated by spin-coating method, and other layers were fabricated by vacuum deposition. All devices showed EL spectra that match the PL spectra of the dendrimer neat films, while a slight red shift was observed, probably due to the difference in electronic excitation and photoexcitation. The maximum EQE (EQE_{max}) of the devices reached 4.1% for G2TAZ, 2.9% for TPPhG2TAZ, and 5.2% for PFG2TAZ. These devices were not fully optimized, so that the EQE_{max} values did not reach the theoretical limit that can be estimated from the PLQY of the neat film. However, the EQE_{max} value of G2TAZ is comparable to that described in the previous report.[22a] The device employing PFG2TAZ exhibited the highest EQE_{max} as a consequence of the highest PLQY and efficient TADF properties, whereas TPPhG2TAZ showed the lowest EL performance. These results indicate that the terminal modification enable to tune the PLQY and TADF properties of dendrimers, resulting in the enhancement of OLED performance.

5 | CONCLUSION

TAZ core carbazole dendrimers with bulky substituents (adamantane, tetraphenylphenyl, and phenylfluorene) were

synthesized, and their photophysical properties were investigated. In toluene, all dendrimers showed almost 100% PLQY, and in neat film, PLQY was equal to or higher than that of the unsubstituted G2TAZ, and as high as 81% for PFG2TAZ. As a result, the bulky substituents, such as adamantane and tetraphenylphenyl were unsuitable for suppressing concentration quenching, but phenylfluorene was an ideal substituent. The dendrimers, except AdG2TAZ, have good solubility and film-forming properties. AdG2TAZ has low solubility, resulting in films with aggregated particle and rough surface that is unsuitable for OLED devices. PL lifetime measurements showed that TPPhG2TAZ showed little TADF properties, while the other dendrimers showed efficient TADF properties. A large k_{RISC} due to the energy level matching and small $k_{IC,T}$ due to the ideal isolation could explain the highest PLQY of PFG2TAZ in neat film. The OLED device with PFG2TAZ neat film as emitting layer exhibited EQE_{max} of 5.2% which was the highest compared to G2TAZ and TPPhG2TAZ that showed lower PLQY and TADF efficiency. This study does not only contribute to designing TADF dendrimers but also to designing efficient luminescent materials with minimum concentration quenching.

ACKNOWLEDGMENTS

This work was supported, in part, by JSPS KAKENHI Grant Nos. JP23H02026, JP20KK0316, JP23H03966, JP22H02055, JP21H05405, and JP20H02801, and the Cooperative Research Program of "Network Joint Research Center for Materials and Devices" from MEXT, Japan. This study was also supported by the AIST Nanocharacterization Facility (ANCF) platform as a program of the "Nanotechnology Platform" (Grant Number JPMXP09A21AT0017) and "Advanced Research Infrastructure for Materials and Nanotechnology in Japan (ARIM)" (Grant Number JPMXP1222JI0040) of MEXT, Japan, and Transdisciplinary Energy Research (Q-PIT) through its "ModuleResearch" Program from Kyushu University. The computation was carried out using the computer resource offered under the category of General Projects by Research Institute for Information Technology, Kyushu University. Hiroki Ikebe and Ken Albrecht want to thank Ms. Keiko Ideta for helping with NMR measurements.

CONFLICT OF INTEREST STATEMENT

The authors declare no conflicts of interest.

ORCID

Takuma Yasuda https://orcid.org/0000-0003-1586-4701
Ken Albrecht https://orcid.org/0000-0003-2159-2204

REFERENCES

1. a) C. A. Parker, C. G. Hatchard, *Trans. Faraday Soc.* **1961**, *57*, 1894; b) A. Maciejewski, M. Szymanski, R. P. Steer, *J. Phys. Chem.* **1986**, *90*, 6314; c) M. N. Berberan-Santos, J. M. M. Garcia, *J. Am. Chem. Soc.* **1996**, *118*, 9391.
2. a) A. Endo, M. Ogasawara, A. Takahashi, D. Yokoyama, Y. Kato, C. Adachi, *Adv. Mater.* **2009**, *21*, 4802; b) J. C. Deaton, S. C. Switalski, D. Y. Kondakov, R. H. Young, T. D. Pawlik, D. J. Giesen, S. B. Harkins, A. J. M. Miller, S. F. Mickenberg, J. C. Peters, *J. Am. Chem. Soc.* **2010**, *132*, 9499; c) F. B. Dias, K. N. Bourdakos, V. Jankus, K. C. Moss, K. T. Kamtekar, V. Bhalla, J. Santos, M. R. Bryce, A. P. Monkman, *Adv. Mater.* **2013**, *25*, 3707.
3. a) H. Uoyama, K. Goushi, K. Shizu, H. Nomura, C. Adachi, *Nature* **2012**, *492*, 234; b) H. Wu, X.-C. Fan, H. Wang, F. Huang, X. Xiong, Y.-Z. Shi, K. Wang, J. Yu, X.-H. Zhang. *Aggregate* **2022**, *4*, e243.
4. a) N. Aizawa, A. Matsumoto, T. Yasuda, *Sci. Adv.* **2021**, *7*, eabe5769; b) H. Imahori, Y. Kobori, H. Kaji, *Acc. Mater. Res.* **2021**, *2*, 501.
5. a) R. Braveenth, H. Lee, J. D. Park, K. J. Yang, S. J. Hwang, K. R. Naveen, R. Lampande, J. H. Kwon, *Adv. Funct. Mater.* **2021**, *31*, 2105805; b) J. Han, Y. Chen, N. Li, Z. Huang, C. Yang. *Aggregate* **2022**, *3*, e182.
6. W. Xue, H. Yan, Y. He, L. Wu, X. Zhang, Y. Wu, J. Xu, J. He, C. Yan, H. Meng, *Chem. Eur. J.* **2022**, *28*, e202201006.
7. a) Y. Wada, H. Nakagawa, S. Matsumoto, Y. Wakisaka, H. Kaji, *Nat. Photon.* **2020**, *14*, 643; b) T. Hosokai, H. Matsuzaki, H. Nakanotani, K. Tokumaru, T. Tsutsui, A. Furube, K. Nasu, H. Nomura, M. Yahiro, C. Adachi, *Sci. Adv.* **2017**, *3*, e1603282.
8. a) T. Chatterjee, K. T. Wong, *Adv. Opt. Mater.* **2019**, *7*, 1800565; b) S. Y. Byeon, D. R. Lee, K. S. Yook, J. Y. Lee, *Adv. Mater.* **2019**, *31*, 1803714; c) U. Balijapalli, M. Tanaka, M. Auffray, C. Y. Chan, Y. T. Lee, Y. Tsuchiya, H. Nakanotani, C. Adachi, *ACS Appl. Mater. Interfaces* **2020**, *12*, 9498; d) Park IS, Min H, Yasuda T. *Aggregate* **2021**, *2*, 145.
9. a) J. H. Burroughes, D. D. C. Bradley, A. R. Brown, R. N. Marks, K. Mackay, R. H. Friend, P. L. Burns, A. B. Holmes, *Nature* **1990**, *347*, 539; b) M. C. Gather, A. Köhnen, K. Meerholz, *Adv. Mater.* **2010**, *23*, 233; c) D. Di, A. S. Romanov, L. Yang, J. M. Richter, J. P. H. Rivett, S. Jones, T. H. Thomas, M. A. Jalebi, R. H. Friend, M. Linnolahti, M. Bochmann, D. Credgington, *Science* **2017**, *356*, 159; d) D. Liu, M. Zhang, W. Tian, W. Jiang, Y. Sun, Z. Zhao, B. Z. Tang, *Aggregate* **2022**, *3*, e164.
10. M. Godumala, S. Choi, M. J. Cho, D. H. Choi, *J. Mater. Chem. C* **2019**, *7*, 2172.
11. a) Y. Cho, K. Yook, J. Lee, *Adv. Mater.* **2014**, *26*, 6642; b) Y. Wada, K. Shizu, S. Kubo, K. Suzuki, H. Tanaka, C. Adachi, H. Kaji, *Appl. Phys. Lett.* **2015**, *107*, 18330.
12. a) A. E. Nikolaenko, M. Cass, F. Bourcet, D. Mohamad, M. Roberts, *Adv. Mater.* **2015**, *27*, 7236; b) J. Luo, G. Xie, S. Gong, T. Chen, C. Yang, *Chem. Commun.* **2016**, *52*, 2292; c) Z. Ren, R. S. Nobuyasu, F. B. Dias, A. P. Monkman, S. Yan, M. R. Bryce, *Macromolecules* **2016**, *49*, 5452; d) S. Lee, T. Yasuda, H. Komiyama, J. Lee, C. Adachi, *Adv. Mater.* **2016**, *28*, 4019; e) P. Khammultri, W. Kitisriworaphan, P. Chasing, S. Namuangruk, T. Sudyoadsuk, V. Promarak, *Polym. Chem.* **2021**, *12*, 1030; (f) T. Jiang, Y. Liu, Z. Ren, S. Yan, *Polym. Chem.* **2020**, *11*, 1555; g) Shao S, Wang L. *Aggregate* **2020**, *1*, 45.
13. a) K. Albrecht, K. Matsuoka, K. Fujita, K. Yamamoto, *Angew. Chem. Int. Ed.* **2015**, *54*, 5677; b) Y. Li, G. Xie, S. Gong, K. Wu, C. Yang, *Chem. Sci.* **2016**, *7*, 5441; c) J. Luo, S. Gong, Y. Gu, T. Chen, Y. Li, C. Zhong, G. Xie, C. Yang, *J. Mater. Chem. C* **2016**, *4*, 2442; d) X. Wang, J. Hu, J. Lv, Q. Yang, H. Tian, S. Shao, L. Wang, X. Jing, F. Wang, *Angew. Chem. Int. Ed.* **2021**, *60*, 16585.
14. a) D. A. Tomalia, H. Baker, J. Dewald, M. Hall, G. Kallos, S. Martin, J. Roeck, J. Ryder, P. Smith, *Polym. J.* **1985**, *17*, 117; b) D. Astruc, E. Boisselier, C. Ornelas, *Chem. Rev.* **2010**, *110*, 1857.
15. a) A. W. Freeman, S. C. Koene, P. R. L. Malenfant, M. E. Thompson, J. M. J. Fréchet, *J. Am. Chem. Soc.* **2000**, *122*, 12385; b) P. L. Burn, S.-C. Lo, I. D. W. Samuel, *Adv. Mater.* **2007**, *19*, 1675; c) T. Qin, G. Zhou, H. Scheiber, R. E. Bauer, M. Baumgarten, C. E. Anson, E. J. W. List, K. Müllen, *Angew. Chem.* **2008**, *120*, 8416.
16. a) Q. Zhang, Y. F. Hu, Y. X. Cheng, G. P. Su, D. G. Ma, L. X. Wang, X. B. Jing, F. S. Wang, *Synth. Met.* **2003**, *137*, 1111; b) P. Moonsin, N. Prachumrak, R. Rattanawan, T. Keawin, S. Jungsuttiwong, T. Sudyoadsuk, V. Promarak, *Chem. Commun.* **2012**, *48*, 3382; c) K. Albrecht, Y. Kasai, A. Kimoto, K. Yamamoto, *Macromolecules* **2008**, *41*, 3793.
17. a) J. Li, T. Zhang, Y. Liang, R. Yang, *Adv. Funct. Mater.* **2012**, *23*, 619; b) K. Albrecht, K. Matsuoka, K. Fujita, K. Yamamoto, *Mater. Chem. Front.* **2018**, *2*, 1097.
18. a) K. Albrecht, Y. Kasai, K. Yamamoto, *J. Inorg. Organomet. Polym.* **2008**, *19*, 118; b) S. Gambino, S. G. Stevenson, K. A. Knights, P. L. Burn, I. D. W. Samuel, *Adv. Funct. Mater.* **2009**, *19*, 317.
19. a) K. Albrecht, K. Yamamoto, *J. Am. Chem. Soc.* **2009**, *131*, 2244; b) N. D. McClenaghan, R. Passalacqua, F. Loiseau, S. Campagna, B. Verheyde, A. Hameurlaine, W. Dehaen, *J. Am. Chem. Soc.* **2003**, *125*, 5356; c) K. Mutkins, S. S. Y. Chen, A. Pivrikas, M. Aljada, P. L. Burn, P. Meredith, B. J. Powell, *Polym. Chem.* **2013**, *4*, 916; d) K. Albrecht, R.

Pernites, M. Felipe, R. C. Advincula, K. Yamamoto, *Macromolecules* **2012**, *45*, 1288.
20. a) X. Ban, W. Jiang, K. Sun, B. Lin, Y. Sun, *ACS Appl. Mater. Interfaces* **2017**, *9*, 7339; b) J. Luo, S. Gong, Y. Gu, T. Chen, Y. Li, C. Zhong, G. Xie, C. Yang, *J. Mater. Chem. C* **2016**, *4*, 2442.
21. a) H. Tanaka, K. Shizu, H. Miyazaki, C. Adachi, *Chem. Commun.* **2012**, *48*, 11392; (b) T. Serevičius, T. Nakagawa, M.-C. Kuo, S.-H. Cheng, K.-T. Wong, C.-H. Chang, R. C. Kwong, S. Xia, C. Adachi, *Phys. Chem. Chem. Phys.* **2013**, *15*, 15850; c) S. Hirata, Y. Sakai, K. Masui, H. Tanaka, S. Y. Lee, H. Nomura, N. Nakamura, M. Yasumatsu, H. Nakanotani, Q. Zhang, K. Shizu, H. Miyazaki, C. Adachi, *Nature Mater.* **2014**, *14*, 330; d) D. Liu, D. Li, H. Meng, Y. Wang, L. Wu, *J. Mater. Chem. C* **2019**, *7*, 12470.
22. a) K. Albrecht, K. Matsuoka, D. Yokoyama, Y. Sakai, A. Nakayama, K. Fujita, K. Yamamoto, *Chem. Commun.* **2017**, *53*, 2439; b) T. Matulaitis, P. Imbrasas, N. A. Kukhta, P. Baronas, T. Bučiūnas, D. Banevičius, K. Kazlauskas, J. V. Gražulevičius, S. Juršėnas, *J. Phys. Chem. C* **2017**, *121*, 23618; c) D. Sun, E. Duda, X. Fan, R. Saxena, M. Zhang, S. Bagnich, X. Zhang, A. Köhler, E. Zysman-Colman, *Adv. Mater.* **2022**, *34*, 2110344.
23. a) K. Matsuoka, K. Albrecht, A. Nakayama, K. Yamamoto, K. Fujita, *ACS Appl. Mater. Interfaces* **2018**, *10*, 33343; b) X. Ban, A. Zhu, T. Zhang, Z. Tong, W. Jiang, Y. Sun, *ACS Appl. Mater. Interfaces* **2017**, *9*, 21900.
24. W.-L. Tsai, M.-H. Huang, W.-K. Lee, Y.-J. Hsu, K.-C. Pan, Y.-H. Huang, H.-C. Ting, M. Sarma, Y.-Y. Ho, H.-C. Hu, C.-C. Chen, M.-T. Lee, K.-T. Wong, C.-C. Wu, *Chem. Commun.* **2015**, *51*, 13662.
25. K. Albrecht, E. Hisamura, M. Furukori, Y. Nakayama, T. Hosokai, K. Nakao, H. Ikebe, A. Nakayama, *Polym. Chem.* **2022**, *13*, 2277.
26. A. Klapars, J. C. Antilla, X. Huang, S. L. Buchwald, *J. Am. Chem. Soc.* **2001**, *123*, 7727.
27. M. Numata, (Idemitsu Kosan Co., Ltd.), JP. P2013-108015A, **2013**.
28. Q. Xiang, X. Sun, G. Zhu, H. Sun, Y. Wan, Z. Si, Q. Duan, *Eur. J. Inorg. Chem*. **2012**, *2012*, 4012.
29. L. H. Xie, X. Y. Hou, Y. R. Hua, C. Tang, F. Liu, Q. L. Fan, W. Huang, *Org. Lett.* **2006**, *8*, 3701.
30. a) T. Ishizone, H. Tajima, S. Matsuoka, S. Nakahama, *Tetrahedron Lett.* **2001**, *42*, 8645; b) T. Ishizone, *Kobunshi* **2004**, *53*, 342; c) L. J. Mathias, G. L. Tullos, *Polymer* **1996**, *37*, 3771; d) D. Plaza-Lozano, B. Comesaña-Gándara, M. de la Viuda, J. G. Seong, L. Palacio, P. Prádanos, J. G. de la Campa, P. Cuadrado, Y. M. Lee, A. Hernández, C. Alvarez, A. E. Lozano, *Mater. Today Commun.* **2015**, *5*, 23.
31. a) J. F. Ambrose, R. F. Nelson, *J. Electrochem. Soc.* **1968**, *115*, 1159; b) J. F. Ambrose, L. L. Carpenter, R. F. Nelson, *J. Electrochem. Soc.* **1975**, *122*, 876.
32. C. Reichardt, *Chem. Rev*. **1994**, *94*, 2319.
33. K. Masui, H. Nakanotani, C. Adachi, *Org. Electron.* **2013**, *14*, 2721.
34. M. Furukori, Y. Nagamune, Y. Nakayama, T. Hosokai, *J. Mater. Chem. C* **2023**, *11*, 4357.
35. D. de Sa Pereira, D. R. Lee, N. A. Kukhta, K. H. Lee, C. L. Kim, A. S. Batsanov, J. Y. Lee, A. P. Monkman, *J. Mater. Chem. C* **2019**, *7*, 10481.

SUPPORTING INFORMATION

Additional supporting information can be found online in the Supporting Information section at the end of this article.

How to cite this article: H. Ikebe, K. Nakao, E. Hisamura, M. Furukori, Y. Nakayama, T. Hosokai, M. Yang, G. Liu, T. Yasuda, K. Albrecht, *Aggregate* **2024**, *5,* e405. https://doi.org/10.1002/agt2.405